AAC
Journals.ASM.org

Milbemycins: More than Efflux Inhibitors for Fungal Pathogens

Luis Vale Silva,[a] Maurizio Sanguinetti,[b] Patrick Vandeputte,[a,c] Riccardo Torelli,[b] Bertrand Rochat,[d] Dominique Sanglard[a]

Institute of Microbiology, University of Lausanne and University Hospital Center, Lausanne, Switzerland[a]; Institute of Microbiology, Università Cattolica del Sacro Cuore, Rome, Italy[b]; Groupe d'Etude des Interactions Hôte-Pathogène, UPRES-EA 3142, Universitè d'Angers, Centre Hospitalier Universitaire, Angers, France[c]; Quantitative Mass Spectrometry Facility, University of Lausanne and University Hospital Center, Lausanne, Switzerland[d]

Existing antifungal agents are still confronted to activities limited to specific fungal species and to the development of resistance. Several improvements are possible either by tackling and overcoming resistance or exacerbating the activity of existing antifungal agents. In *Candida glabrata*, azole resistance is almost exclusively mediated by ABC transporters (including *C. glabrata CDR1* [*CgCDR1*] and *CgCDR2*) via gain-of-function mutations in the transcriptional activator *CgPDR1* or by mitochondrial dysfunctions. We also observed that azole resistance was correlating with increasing virulence and fitness of *C. glabrata* in animal models of infection. This observation motivated the re-exploitation of ABC transporter inhibitors as a possible therapeutic intervention to decrease not only the development of azole resistance but also to interfere with the virulence of *C. glabrata*. Milbemycins are known ABC transporter inhibitors, and here we used commercially available milbemycin A3/A4 oxim derivatives to verify this effect. As expected, the derivatives were inhibiting *C. glabrata* efflux with the highest activity for A3 oxim below 1 μg/ml. More surprising was that oxim derivatives had intrinsic fungicidal activity above 3.2 μg/ml, thus highlighting effects additional to the efflux inhibition. Similar values were obtained with *C. albicans*. Our data show that the fungicidal activity could be related to reactive oxygen species formation in these species. Transcriptional analysis performed both in *C. glabrata* and *C. albicans* exposed to A3 oxim highlighted a core of commonly regulated genes involved in stress responses, including genes involved in oxidoreductive processes, protein ubiquitination, and vesicle trafficking, as well as mitogen-activated protein kinases. However, the transcript profiles contained also species-specific signatures. Following these observations, experimental treatments of invasive infections were performed in mice treated with the commercial A3/A4 oxim preparation alone or in combination with fluconazole. Tissue burden analysis revealed that oxims on their own were able to decrease fungal burdens in both *Candida* species. In azole-resistant isolates, oxims acted synergistically *in vivo* with fluconazole to reduce fungal burden to levels of azole-susceptible isolates. In conclusion, we show here the potential of milbemycins not only as drug efflux inhibitors but also as effective fungal growth inhibitors in *C. glabrata* and *C. albicans*.

Superficial and life-threatening systemic fungal infections have been increasing over the last 2 decades. The majority of systemic fungal infections are caused by *Candida*, *Aspergillus*, and *Cryptococcus* species, but *Candida albicans* and non-*albicans Candida* species still account for most of the infections. A few treatment options exist in medical practice, including the use of at least four antifungal chemical classes (azoles, candins, pyrimidine analogues, and polyenes). Emergence of antifungal resistance is a consequence of long-term use of these agents, which is occurring in most immunocompromised patients with HIV or undergoing organ transplants or cancer chemotherapy (1). Clinical criteria can define antifungal resistance, and this has been achieved by the setting of Clinical Break Points (CPB) which indicate a drug concentration for a given fungal pathogen above/under which failure/success of a therapy can be expected (2). For example and according to these criteria, antifungal resistance for azoles is currently the highest for *C. glabrata* among other *Candida* spp. and accounts for 10 to 20% of the *C. glabrata* population (3, 4). This yeast species is ranked as second after *C. albicans* among bloodstream isolates. Recent studies report in several institutions an epidemiological shift of *C. glabrata* at the expense of *C. albicans*, but the reasons behind this phenomenon are still unexplained (4).

Antifungal resistance involves different mechanisms, including principally enhanced drug efflux and target alterations by active-site mutations or overexpression (5). In *C. glabrata*, one of the prominent resistance mechanisms invokes the participation of multidrug transporters of the ABC transporter family (*CgCDR1*, *CgCDR2*, and *CgSNQ2*) (6–8). We and others have found that these transporters are upregulated in azole-resistant isolates with an MIC higher than 16 μg/ml for fluconazole. The upregulation is associated with mutations, so-called gain-of-function (GOF) mutations, in a transcription factor of the Zn2-Cys6 family, *CgPDR1* (1, 9–13). In *C. albicans*, antifungal resistance is multifactorial and involves the participation of efflux transporters, target mutations, compensatory mutations, and genome rearrangements (5). As in the case of *C. glabrata*, mutations in the transcription factors *TAC1*, *MRR1*, and *UPC2* result in the upregulation of target genes participating to the development of azole resistance (14–18). The resistance levels achieved by *C. glabrata* and *C. albicans* address the need to overcome and avoid this phenomenon. Several concepts have been proposed in the past and utilize as basic principle the combination of one antifungal with another compound in order

Received 11 October 2012 Returned for modification 3 November 2012
Accepted 25 November 2012
Published ahead of print 3 December 2012
Address correspondence to Dominique Sanglard, dominique.sanglard@chuv.ch.
L.V.S. and M.S. contributed equally to this article.
Supplemental material for this article may be found at http://dx.doi.org/10.1128/AAC.02040-12.

doi:10.1128/AAC.02040-12

to increase antifungal activity (19, 20). Given the importance of ABC-transporters for the development of azole resistance both in *C. glabrata* and *C. albicans*, one possible option to tackle resistance could be the use of transporter inhibitors. In cancer research, human P-gp, which are functional homologs of fungal ABC transporters, are important mediators of resistance to many anticancer drugs. A wide range of P-gp-inhibitory compounds identified include natural and synthetic polymers, P-gp substrates (such as FK506), calcium channel modulator (verapamil), calmodulin inhibitors, and quinine analogs (21). Consequently, implementing the concept of combination therapy using an efflux inhibitor in order to increase the activity of fluconazole, a drug still widely used to treat fungal infections, seems an adequate strategy for overcoming resistance development in *C. glabrata*.

Drug resistance acquisition can also be associated to fitness costs in several microbial systems (22). In *C. glabrata*, however, we found that azole resistance was on the contrary resulting in enhanced virulence and fitness in animal models. This feature was dependent on the presence of a GOF mutation in *CgPDR1* (9). Recently, we found that this effect could be mediated partially by the ABC transporter *CgCDR1*, which is upregulated to variable levels in azole-resistant isolates in *C. glabrata* (23).

Since *CgCDR1* plays an important role in the development of azole resistance and that it can also contribute to increase virulence and fitness of *C. glabrata*, we reasoned that ABC transporters inhibitors such as milbemycins could be of potential therapeutic interest. We demonstrate here that specific milbemycin derivatives not only exhibit expected activities as efflux inhibitors but also that they possess intrinsic antifungal and fungicidal activities. Here we show that experimental treatments of *C. glabrata* infections by combination therapy are feasible and expanded this idea to *C. albicans* infections. Lastly, we perform transcriptional profiling of both *Candida* species exposed to milbemycins in order to understand the basis for their unexpected antifungal activity.

TABLE 1 Strains used in this study

Isolate	Characteristics	Fluconazole MIC (μg/ml)[a]	Source or reference
SC5314	Wild type *C. albicans* isolate	0.25	24
DSY294	Clinical *C. albicans* isolate, azole susceptible	0.5	25
DSY296	Clinical *C. albicans* isolate, azole resistant	128	25
DSY2321	Clinical *C. albicans* isolate, azole susceptible	0.25	26
DSY2323	Clinical *C. albicans* isolate, azole resistant	32	26
DSY741	Clinical *C. albicans* isolate, azole susceptible	0.25	27
DSY742	Clinical *C. albicans* isolate, azole resistant	16	27
DSY562	Clinical *C. glabrata* isolate, azole susceptible	4	9
DSY565	Clinical *C. glabrata* isolate, azole resistant	128	9
DSY529	Clinical *C. glabrata* isolate, azole susceptible	8	6
DSY530	Clinical *C. glabrata* isolate, azole resistant	128	6
DSY726	Clinical *C. glabrata* isolate, azole susceptible	4	9
DSY727	Clinical *C. glabrata* isolate, azole resistant	128	9

[a] MICs were measured by the EUCAST protocol (28) as described in Materials and Methods.

MATERIALS AND METHODS

Strains, media, and drugs. The *C. albicans* strains used in the present study are listed in Table 1. Yeast strains were grown in liquid YEPD complete medium (1% Bacto peptone [Difco], 0.5% yeast extract [Difco], 2% glucose [Fluka]). To grow the strains on solid media, 2% agar (Difco) was added. *Escherichia coli* DH5α was used as a host for plasmid construction and propagation. DH5α cells were grown in Luria-Bertani (LB) broth or on LB plates, which were supplemented with ampicillin (0.1 mg/ml) when required. Fluconazole was obtained from Sigma. Milbemycins were obtained from Novartis Animal Health (Basel, Switzerland).

Drug susceptibility testing. Susceptibility assays were performed according to the standard broth microdilution protocols Edef. 7.1 (Subcommittee on Antifungal Susceptibility Testing of the ESCMID European Committee for Antimicrobial Susceptibility Testing [AFST-EUCAST]) (28). Briefly, serial 2-fold dilutions of fluconazole in RPMI 1640 broth (with L-glutamine, without bicarbonate and with phenol red as the pH indicator; Sigma), supplemented with 2%, (wt/vol) of D-glucose for Edef. 7.1, were distributed in 50-μl volumes at four times the final desired concentration into the wells of flat-bottom microtiter plates. Fluconazole final concentrations ranged from 128 to 0.25 μg/ml. Cell suspensions were prepared in sterile saline solution from overnight cultures of yeast strains at 35°C in Sabouraud dextrose agar plates. The suspensions were diluted in the test medium and added in 150-μl volumes to the drug solutions in the microtiter plates to yield final inoculum sizes of 0.5 to 2.5×10^5 cells/ml. Drug-free cultures and sterility controls were included in each microtiter plate. The plates were incubated at 35°C, and the MIC values were read after 24 h by measuring the absorbance using a spectrophotometric microdilution plate reader set at 450 nm. Checkerboard tests were performed with a similar procedure but including serial dilutions of milbemycins in a 50-μl volume at four times the final desired concentration for each fluconazole-containing well and with final concentrations ranging from 0.8 to 25.6 μg/ml. Milbemycins were first diluted in dimethyl sulfoxide (DMSO) and diluted accordingly. DMSO concentration in final suspensions was 0.8%. The cell suspensions were added in 100-μl volumes to the drug solutions to obtain final inoculum sizes of 0.5 to 2.5×10^5 cells/ml.

The fractional inhibitory concentration (FIC) index for a drug combination in the checkerboard method is the minimum ΣFIC obtained with the following equation: $\Sigma FIC = FIC_A + FIC_B = (C_{FLC}/MIC_{FLC}) + (C_{Mil}/MIC_{Mil})$, where MIC_{FLC} and MIC_{Mil} are the MICs of fluconazole and the tested milbemycin when tested alone, and C_{FLC} and C_{Mil} are the concentrations of fluconazole and the tested milbemycin resulting in at least 50% growth inhibition in a given well in the 96-well microtiter plate. Interactions were categorized according to the method of Te Dorsthorst et al. (29) by the following rules: synergism (FIC, ≤0.5), additivity (FIC, >0.5 to ≤1), and indifference (FIC, >1 to <4).

Efflux of rhodamine 6G. A whole cells rhodamine 6G (R6G) efflux assay, adapted from a previously developed protocol, was used to measure the drug efflux capacity of *C. albicans* and *C. glabrata* isolates (30). Each fungal species required a specific procedure for cell preparation. For *C. albicans*, cell cultures grown overnight in YEPD were diluted in 5 ml of fresh medium and allowed to grow at 30°C under constant agitation to a density of 2×10^7 cells/ml. Cells were centrifuged, washed in 5 ml of phosphate-buffered saline (PBS; pH 7), and resuspended in 2 ml of PBS. These suspensions were incubated for 1 h at 30°C under constant agitation to energy-deprived cells, and R6G was next added at a concentration of 10 μg/ml. The incubation was continued for 1 h to allow R6G accumulation. After this incubation time, cells were sedimented by centrifugation, washed with PBS at 4°C, and resuspended in a final volume of 300 μl of PBS. For *C. glabrata*, overnight cultures were diluted to 2×10^7 cells/ml in

50 ml of YEPD and agitated for 4 h at 30°C. Cells were next washed twice with PBS and resuspended in PBS at a 2% (wet weight) concentration. R6G was added to a 10 μM end concentration together with 2 mM deoxyglucose. After 1 h of incubation at 30°C, the cells were washed twice with PBS and resuspended to a concentration of 10^8 cells/ml.

Fifty-microliter portions of individual suspensions were diluted in 150 μl of PBS and divided into aliquots into a 96-well microtiter plate, which was then placed in a SpectraMax Gemini fluorimeter (Molecular Devices, Sunnyvale, CA, USA) with a temperature control set at 30°C. Baseline emission of fluorescence (excitation wavelength, 344 nm; emission wavelength, 555 nm) was recorded for 5 min as relative fluorescence units (RFU), and D-glucose was next added to each strain at a final concentration of 1% (wt/vol) to initiate R6G efflux. As negative controls, no glucose was added to a series of separate aliquots of each strain. The data points were recorded in duplicate for 60 min in 1-min intervals.

Efflux inhibition with milbemycins was carried out by adding the different compounds to each yeast sample. The milbemycin-yeast cell mixture was incubated for 10 min at room temperature before initiation of efflux experiments.

MitoSOX Red staining. Intracellular reactive oxygen species (ROS) production was examined using MitoSOX Red (Molecular Probes). MitoSOX Red is a lipid soluble cation that accumulates in the mitochondrial matrix, where it can be oxidized to a fluorescent product by superoxide. Yeast strains from initial concentration of 2×10^6 cells/ml were grown in RPMI medium containing 10 μg of A3Ox/ml. After 1 h of incubation, 500-μl aliquots were washed twice with PBS and incubated in the dark for 20 min in 2.5 μM MitoSOX Red. The cells were washed three times with PBS and resuspended in PBS, and the percentage of cells positively stained with MitoSOX Red was determined by fluorescence microscopy using a Zeiss Axioplan 2 fluorescence microscope. Images were recorded using a Visitron Systems HistoScope Camera and VisiView Imaging Software. Fluorescence of cells was also determined using a FLUOstar OMEGA microplate reader (BMG) with excitation and emission wavelengths of 510 and 580 nm, respectively.

Construction of *Candida* microarrays. *C. glabrata* microarrays were designed according to the Agilent eArray Design guidelines as previously described (23), and custom arrays were manufactured in the 8×15 K format by Agilent Technologies. *C. albicans* microarrays were also manufactured by Agilent Technologies; however, the array design (design ID 037331) was obtained from Synnott et al. (31). A total of 6,101 genes (including 12 mitochondrial genes) are represented by two sets of probes, both spotted in duplicate. Four copies of each array were printed on a 4×44 K format.

cRNA synthesis, one-color labeling, and array hybridization. Sample preparation was performed on biological quadruplicate cultures of the *C. glabrata* strain DSY562 and biological triplicate for the *C. albicans* strain SC5314. Log-phase cultures at 35°C with agitation in RPMI 1640 medium with 2% D-glucose were treated for 1 h in the same conditions with either 10 μg of milbemycin A3 oxim/ml or the DMSO solvent. Total RNA was extracted after mechanical disruption of the cells with glass beads by a phenol-chloroform-lithium chloride procedure, as previously described (32). The integrity of the input RNA template was determined prior to labeling or amplification using an Agilent RNA 6000 Nano LabChip kit and 2100 BioAnalyzer (Agilent Technologies). Agilent's One-Color Quick Amp labeling kit (Agilent Technologies) was used to generate fluorescent cRNA as previously described (32). Briefly, a spike mix and T7 promoter primers were added to 400 ng of total RNA from each sample. cDNA synthesis was promoted by Moloney murine leukemia virus reverse transcriptase in the presence of deoxynucleoside triphosphates and RNaseOUT. Next, cRNA was produced from this first reaction with T7 RNA polymerase, which simultaneously amplifies target material and incorporates cyanine 3-labeled CTP. The labeled cRNAs were purified with an RNeasy minikit (Qiagen) and quantified using a NanoDrop ND-1000 UV/VIS spectrophotometer. A total of 600 ng of Cy3-labeled cRNAs from each sample were fragmented and hybridized for 17 h at 65°C to specific subarrays of the 8×15 K or 4×44 K format using a gene expression hybridization kit (Agilent Technologies) and a gasket slide.

Microarray data analysis. Slides were washed and processed according to the Agilent 60-mer Oligo microarray processing protocol and scanned on an Agilent microarray scanner G2565BA (Agilent Technologies). The data were extracted from the images with feature extraction (FE) software (Agilent Technologies). Each slide was processed with spike quality controls to establish the dynamic range of signals which fitted a minimum R^2 value of 0.99. The FE software flags outlier features (the percentages ranged from 0.01 to 0.15% of signals overall for cRNA hybridizations) and detects and removes spatial gradients and local backgrounds. The data were normalized using a combined rank consistency filtering with Lowess intensity normalization. The gene expression values obtained with FE software were imported into GeneSpring 11 software (Agilent Technologies) for preprocessing and data analysis. For interarray comparisons, a linear scaling of the data was performed using the quantile normalization of one-color signal values of noncontrol probes on the microarray. The expression of each gene was normalized by its median expression across all samples. Statistical analyses were performed using unpaired *t* tests and a corrected *P* value of 0.05 was chosen as the cutoff for significance. Changes in expression for each gene of at least 2-fold between treated and nontreated samples were considered significant. Microarray data can be retrieved at the Gene Expression Omnibus NCBI site under the accession number GSE40232. Validation of gene expression results from microarray analysis was performed by quantitative real-time PCR (qPCR) as detailed below.

qPCR. RNA sample preparation was performed as described above for microarray experiments. RNA samples were treated with RNase-free DNase (DNA-free; Ambion) to remove any contaminating genomic DNA and reverse transcribed using random hexamers as the priming method (Transcriptor First-Strand cDNA synthesis kit; Roche). Expression levels of *C. glabrata* target genes (*ERG4*, *MET3*, *YPS1*, and *YPS3*) and the *C. albicans* genes (*HXT6*, *WOR1*, and *OPT5*) were determined by a SYBR green-based quantitative real-time PCR (MesaBlue qPCR kit for SYBR assay; Eurogentec) in a StepOne Plus real-time thermal cycler (Applied Biosystems). Primers used for *YPS1* and *YPS3* quantification were previously described (23). Primers used for quantification of the remaining genes are listed in Table 2. Relative gene expression in milbemycin A3 oxim-treated samples in comparison to nontreated controls was determined from *CgTEF3*-normalized expression levels for *C. glabrata* and *ACT1* for *C. albicans*.

Animal experiments. Female BALB/c mice (20 to 25 g) were purchased from Harlan Italy S.r.l (San Pietro al Natisone, Udine, Italy) and inbred in-house. The mice were housed in filter-top cages with free access to food and water. To establish *C. glabrata* infection, mice were injected into their lateral vein with saline suspensions of the *C. glabrata* strains (each in a volume of 200 μl).

Groups of 10 mice were established for each yeast strain. For tissue burden experiments, immunocompetent mice were inoculated with 4×10^7 CFU of each *C. glabrata* strains and 7×10^4 CFU of each *C. albicans* strains. After 7 days, mice were sacrificed by use of CO_2 inhalation, and target organs (spleen and kidney) were excised aseptically, weighted individually, and homogenized in sterile saline by using a Stomacher 80 device (Pbi International, Milan, Italy) for 120 s at high speed. Organ homogenates were diluted and plated onto YPD. Colonies were counted after 2 days of incubation at 30°C, and the numbers of CFU g of organ^{-1} were calculated. CFU counts were analyzed with nonparametric Wilcoxon rank-sum tests. A *P* value of <0.05 was considered to be significant.

The milbemycin injectable solution was prepared by adding 1 volume of PEG 400 to 2 volumes of a milbemycin DMSO solution (0.2 mg/ml) in order to obtain a 0.1-mg/ml solution with DMSO/PEG 400 ratio of 2:1. The DMSO/PEG solution was injected in a 100-μl volume intraperitoneally each day. Fluconazole was injected intraperitoneally at dosages of 100 mg/kg/day dosage for *C. glabrata* and of 3 mg/kg/day for *C. albicans*.

TABLE 2 Primers usedin this study

Primer	Sequence (5′-3′)	Source or reference
CgMET3-F	GGACGCCATCCAGCTGCCA	This study
CgMET3-R	AGCGGCACGCACGGTCAA	This study
CgERG4_F	ATTGACCCACTTGAAGA	This study
CgERG4_R	GGCACAAGTCATTATTCT	This study
CgTEF3-F	CGGTGGTAAGAAGAAGAA	This study
CgTEF3-R	AGAAACGTAAGCATCACC	This study
CgYPS1a	CCTCCGCCAGATTGTGGCATG	23
CgYPS1b	CTCGAACAGAGCCGGTTACTA	23
CgYPS3a	CGACGACCCATCCCCAGGCTC	23
CgYPS3b	ACTTAGCTCTTCATGGTAACG	23
CgACT1a	GTGTGAATAACCGCTGCGATACT	23
CgACT1b	TGCCCACCACTCCTAACTCATAAT	23
WOR1-qPCR-F	TCCCGACGACGAGTACGACCA	This study
WOR1-qPCR-R	CCAGTCGCAAGCAACATTGGACC	This study
TNA1-qPCR-F	TGCTGCCTCGGGAGCCATTG	This study
TNA1-qPCR-R	AGAATGGCGCAACCAGCAGTT	This study
OPT5-qPCR-F	TCTTGGGTTTGGGCTTTCTGGA	This study
OPT5-qPCR-R	TGCTTTCACTTCAGGCGACA	This study
HXT6-qPCR-F	GGGCCTTGTGTTTGCTTGGTGG	This study
HXT6-qPCR-R	TGCAGGGTCCTCTGGAGAAA	This study
ACT1-RT-F	GTTCCCAGGTATTGCTGAAC	33
ACT1-RT-R	CAATGGATGGACCAGATTCG	33

RESULTS

Inhibition profiles with milbemycins. Several milbemycin derivatives are known to exert an inhibition of drug efflux in fungi by targeting the class of ABC transporters (21). Here, we tested the properties of two different milbemycin derivatives (milbemycin A3 and A4), as well as their oxim derivatives which are widely used in veterinary practice as antiparasitic drugs (34). We used an efflux assay based on fluorophore rhodamine 6G (R6G)-loaded cells and a real-time recording of effluxed compound. Milbemycins A3 and A4 (referred here as A3 and A4) as well as their oxim derivatives (referred here as A3Ox and A4Ox) were used at different concentrations to estimate their inhibition capacities. As observed in Fig. 1A and B, R6G efflux in the azole-susceptible isolate DSY562 and the azole-resistant isolate DSY565, respectively, could be stimulated by glucose addition but was gradually decreased with increasing concentrations of A3Ox, this derivative taken as an illustrative example. One can observe that A3Ox was more effective at inhibiting R6G efflux in DSY562 compared to DSY565. This difference reflects that DSY565 contains higher *CgCDR1* levels compared to DSY562 and that higher A3Ox concentrations are needed to cause a decrease in effluxed R6G in DSY565. Additional experiments with a mutant lacking *CgCDR1* (DSY1041) confirmed that the recorded signals were due to R6G efflux (data not shown). To estimate inhibition kinetics of the four different milbemycins in

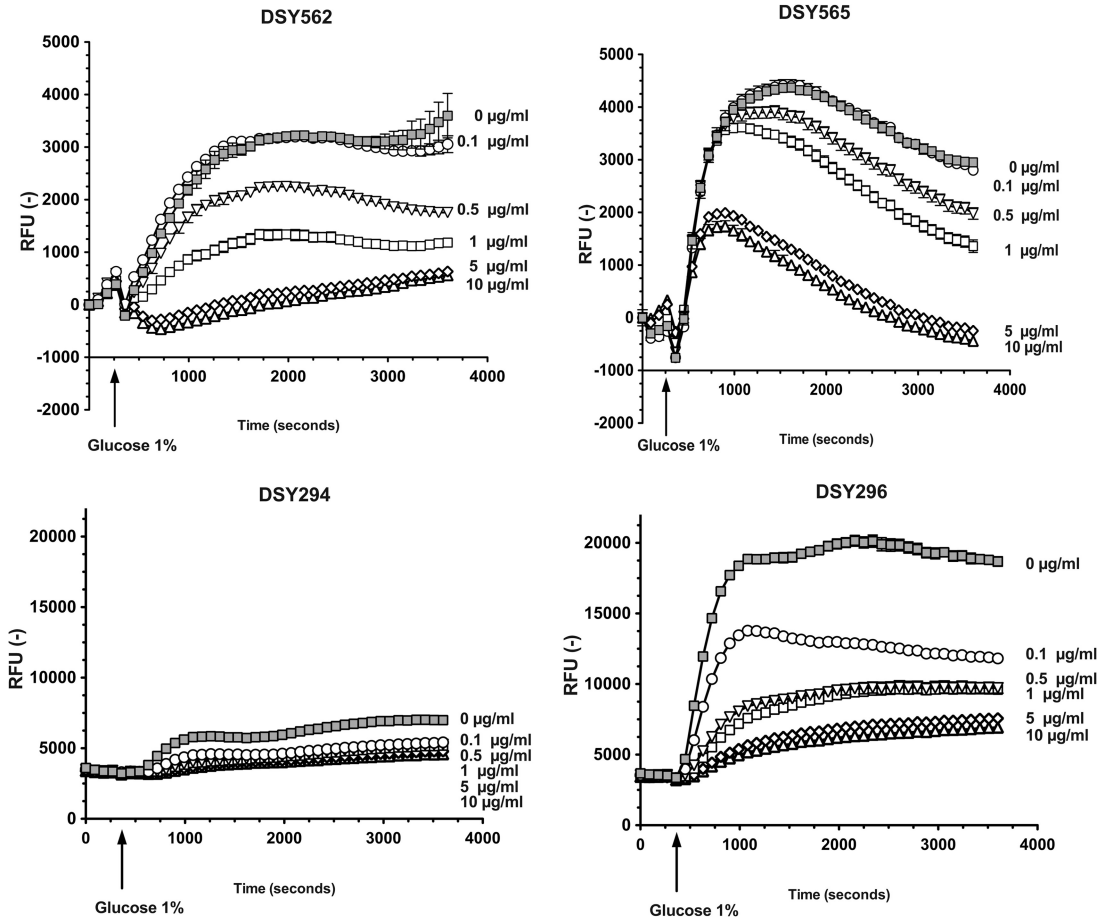

FIG 1 Rhodamine 6G efflux inhibition in *C. glabrata* and *C. albicans*. R6G efflux was recorded over 1 h at regular intervals. Experiments were carried out in triplicates, and mean data (± the standard deviation [SD]) points are shown. Concentrations of A3Ox are shown next to each curve.

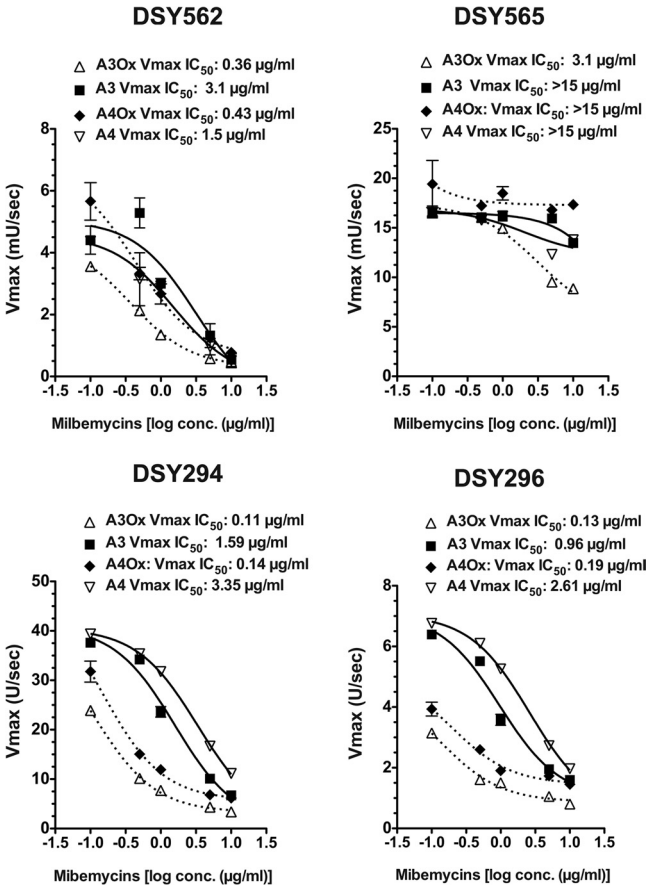

FIG 2 Inhibition characteristics of milbemycins and their oxim derivatives in *C. glabrata* and *C. albicans*. IC_{50}s were calculated using GraphPad Prism software.

DSY562 and DSY565, V_{max} of R6G efflux calculated from RFU values over time were plotted against inhibitor concentrations (Fig. 2). The obtained plots were used to deduce inhibitor concentrations decreasing V_{max} values by 50% (IC_{50}). The obtained IC_{50}s with DSY562 showed that oxims derivatives were more potent than their parent compounds at inhibiting R6G efflux. A3Ox appeared as the most effective substance (V_{max} IC_{50} = 0.36 μg/ml). IC_{50}s obtained with DSY565 were higher than for DSY562. This could be expected since *CgCDR1* is overexpressed in this isolate. However, A3Ox (V_{max} IC_{50} = 3.1 μg/ml) was also the most potent inhibitor of R6G efflux for this isolate, although this value is 10-fold higher than in DSY562.

The same procedures were used to characterize the properties of milbemycins with the azole-susceptible *C. albicans* isolate DSY294 and its azole-resistant parent DSY296. The azole-resistant isolate of this clinical pair upregulates the ABC transporters *CDR1* and *CDR2*, which is one of the mechanisms contributing to azole resistance (25, 26). As observed in Fig. 1, milbemycins could decrease R6G efflux in a concentration-dependent manner. V_{max} IC_{50}s revealed that oxim derivatives possessed the highest inhibition capacity compared to parent compounds (Fig. 2), which was similar to that observed in *C. glabrata*.

Taken together, our results demonstrate that milbemycins A3 and A4 and their oxim derivatives were able to inhibit drug efflux in *C. glabrata* and *C. albicans* and that oxim derivatives exhibited the highest inhibitory capacity.

Combination of milbemycins with fluconazole *in vitro*. Given that A3, A4, and their oxim derivatives can inhibit drug efflux, we expected that fluconazole MICs could be reduced in their presence. We therefore undertook checkerboard assays with fluconazole and each milbemycin compound to estimate fractional inhibitory concentration (FIC) indexes between both drugs. As shown in Fig. 3, we first observed that A3Ox had an antifungal effect on both *C. glabrata* DSY562 and DSY565 (MIC = 6.4 μg/ml, Table 3). This effect was less pronounced for the parent derivative A3 (MIC = 25.6 μg/ml, Table 3). A4Ox and A4 were less active than A3 derivatives, but again the A4Ox was the most active compound (MIC = 25.6 μg/ml, Table 3). FIC indexes were calculated for each drug combination (Table 4) and synergistic and additive effects were made visible in the checkerboard (Fig. 3: white area: synergistic interactions; red area: additive interactions). The 3-color heat map shown in Fig. 3 illustrates drug combinations resulting in cutoff 50% growth reduction (blue color) compared to drug-free growth (green color) and those with absence of growth (black color). Inspection of the data shows that milbemycin-fluconazole interactions were almost exclusively additive, with the exception of a synergistic combination with A3Ox in DSY562 (Fig. 3 and Table 4). We found the same intrinsic antifungal activity A3Ox and derivatives in two other pairs of clinical isolates (DSY529/DSY539 and DSY727/DSY728) that were described elsewhere (see Tables 1 and 3). In addition, A3Ox-fluconazole interaction patterns in these isolates were similar than those observed in DSY562/DSY565 (Table 4). Therefore, it is likely that milbemycins act by the same mechanisms in all clinical *C. glabrata* isolates.

Milbemycin-fluconazole interactions were tested with the *C. albicans* strains DSY294 and DSY296 (Table 3 and 4). With *C. albicans*, both the A3Ox and A4Ox derivative exhibited higher activity than their parent compounds, which is slightly different from *C. glabrata*, in which only the A3Ox derivative was highly active. The A3Ox and A4Ox MICs in *C. albicans* had the same value as measured in *C. glabrata* (3.2–6.4 μg/ml). On the opposite to *C. glabrata*, the combination of milbemycins with fluconazole resulted mostly in synergistic interactions (Table 4). A3Ox and other derivatives had the same range of activity in other pairs of *C. albicans* clinical strains including DSY2321/DSY2323 and DSY741/DSY742 (see Tables 1 and 3). Interestingly, the A3Ox-fluconazole interaction was synergistic for DSY2323, while indifferent for DSY742 (Table 4). The likely explanation behind this opposite behavior is that, even if both isolates are azole-resistant, one (DSY2323) has acquired resistance by ABC transporter upregulation (26) while the other (DSY742) by *MDR1* upregulation (27). Since A3Ox targets ABC transporters, it was expected that fluconazole potentiation could only be revealed in strains overexpressing this type of multidrug transporter.

Milbemycin oxims are fungicidal. Since A3Ox exhibits antifungal activity, we addressed whether this compound could decrease survival upon incubation of cells at the supra-MIC of 10 μg/ml. In *C. glabrata*, A3Ox exhibited a clear fungicidal effect: after 24 h of incubation survival of azole-susceptible and azole-resistant cells decreased by 95% compared to the initial inoculum (Fig. 4). Combining fluconazole with A3Ox slightly increased the fungicidal effect of milbemycin. A3Ox had a strong fungicidal effect on the *C. albicans* DSY294 isolate compared to *C. glabrata*

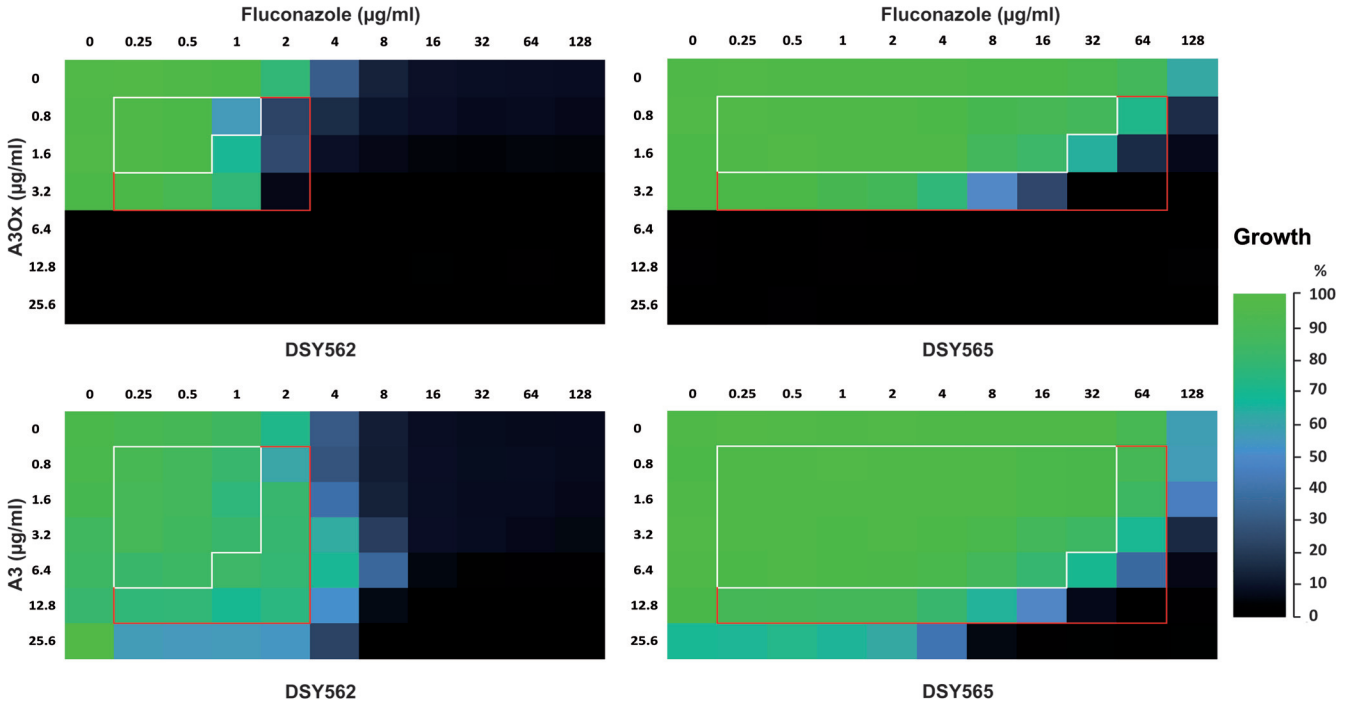

FIG 3 Three-color heat maps of checkerboard MIC tests of A3Ox and A3 with *C. glabrata*. Each box corresponds to relative growth (as compared to drug-free growth) resulting from a specific combination between milbemycins and fluconazole. White-delimited zones correspond to synergistic interactions (FIC index ≤ 0.5). Red-delimited zones correspond to additive interactions (FIC index > 0.5 and ≤ 1). Positive interactions (synergistic or additive) can be visualized when relative growth is ≤50% relative to control (blue to black colored wells). MICs were performed according to EUCAST protocols.

and fluconazole increased this effect substantially. In the azole-resistant *C. albicans* isolate DSY296, A3Ox exhibited still a fungicidal effect (78% decrease in survival compared to inoculum), however it could be still increased by fluconazole, even though this azole had almost no inhibitory effect when used as single drug at the subinhibitory concentration of 64 μg/ml. In conclusion, our data show that A3Ox has fungicidal effect, that the extent of this effect is species-dependent and that fluconazole-A3Ox combinations enhance milbemycin fungicidal effect.

TABLE 3 MICs of *C.glabrata* and *C. albicans* against fluconazole and milbemycins

	MIC (μg/ml)				
Isolate	Fluconazole	A3Ox	A4Ox	A3	A4
C. glabrata					
DSY562	4	6.4	25.6	>25.6	>25.6
DSY565	128	6.4	25.6	25.6	>25.6
DSY529	8	6.4	25.6	>25.6	>25.6
DSY530	128	6.4	25.6	25.6	>25.6
DSY726	4	6.4	25.6	25.6	>25.6
DSY727	128	6.4	25.6	>25.6	>25.6
C. albicans					
DSY294	0.5	6.4	6.4	25.6	25.6
DSY296	128	6.4	3.2	>25.6	12.8
DSY2321	0.25	6.4	6.4	25.6	25.6
DSY2323	32	6.4	3.2	>25.6	>25.6
DSY741	0.25	6.4	6.4	25.6	25.6
DSY742	16	6.4	3.2	>25.6	>25.6
SC5314	0.25	6.4	6.4	25.6	25.6

Given the fungicidal properties of A3Ox, we tested the formation of reactive oxygen species (ROS) during A3Ox exposure using MitoSOX Red, a specific indicator of ROS in mitochondria. As described by Batova et al. (35), the fluorescence intensity of this dye can also distinguish between dead cells (bright fluorescence) and actively ROS-producing cells (low fluorescence). Figure 5A illustrates that ROS could be detected both in *C. glabrata* and *C. albicans*. Quantification of fluorescence signals with MitoSOX Red (Fig. 5B) indicated that A3Ox treatments in both yeast species induced cell death and ROS production. Thus, it is likely that the fungicidal effect of A3Ox involves at some point the formation of ROS, which then could promote the killing of *C. glabrata* and *C. albicans*.

Experimental treatment of invasive candidiasis with milbemycins. Milbemycin oxims (A3Ox and A4Ox) are commercially available. The single substances in the mixture are usually contained in a 2.5:7.5 proportion. We used this commercial preparation since pure substances were available in limited quantities only. Given the efflux-inhibiting capacity of A3Ox and A4Ox, as well as the fungicidal properties of the A3Ox derivative, we tested their potential therapeutic effect in experimental infections in single treatment or in combination with fluconazole. The properties of milbemycin oxims could also have an impact on the virulence of *C. glabrata*, since ABC transporters participate to this phenotype, as described above-mentioned. Animal experiments were carried out with immunocompetent animals and with two different milbemycin regimens, i.e., 0.5 and 2.5 mg/kg/day. Fluconazole was used at a dosage of 100 mg/kg/day. Quantification of milbemycin serum levels at day 7 ranged from 5 to 10 μg/ml (see Fig. S1 in the supplemental material).

TABLE 4 FIC indexes of combination of fluconazole with milbemycins

Isolate	Milbemycin derivative[a]							
	A3Ox		A4Ox		A3		A4	
	Index	Drug effect	Index	Drug effect	Index	Drug effect	Index	Drug effect
C. glabrata								
DSY562	0.4	Synergism	0.8	Additivity	1	Additivity	1	Additivity
DSY565	0.6	Additivity	0.4	Synergism	0.8	Additivity	0.6	Additivity
DSY529	0.5	Synergism	–	–	–	–	–	–
DSY530	0.6	Additivity	–	–	–	–	–	–
DSY726	0.4	Synergism	–	–	–	–	–	–
DSY727	0.6	Additivity	–	–	–	–	–	–
C. albicans								
DSY294	0.4	Synergism	0.4	Synergism	0.3	Synergism	0.3	Synergism
DSY296	0.1	Synergism	0.2	Synergism	0.6	Additivity	0.2	Synergism
DSY2321	0.6	Additivity	–	–	–	–	–	–
DSY2323	0.1	Synergism	–	–	–	–	–	–
DSY741	0.6	Additivity	–	–	–	–	–	–
DSY742	1.1	Indifference	–	–	–	–	–	–

[a] Index, FIC indexes were calculated as described in Materials and Methods. Drug effect, interpretation corresponded to the following definitions: synergism, FIC index ≤ 0.5; additivity, FIC index >0.5 and ≤1; and indifference, FIC index >1 and <4. –, Not tested.

Figure 6 shows results of tissue burdens obtained after 7 days experiments in spleen and kidneys with a 2.5-mg/kg/day milbemycin regimen. Treatment at 0.5 mg/kg/day had similar effects (see Fig. S2 in the supplemental material). Single drug treatments had the following effects on tissue burden (including spleen and kidneys) in infected mice: (i) azole treatment significantly decreased CFU counts only in mice infected with the azole-susceptible isolate DSY562 and (ii) milbemycin treatment decreased CFU counts in mice infected with the two fungal isolates. Combined treatments increased both the milbemycin and fluconazole antifungal effect in animals infected with both strain types. Interestingly, milbemycin and fluconazole treatment reduced tissue burdens of animals infected with the azole-resistant isolate DSY565 to levels comparable to the azole-susceptible isolate DSY562, thus highlighting the power of drug combinations in this animal model.

Similar experiments were carried out with *C. albicans* infections in mice. Both 0.5- and 2.5-mg/kg/day milbemycin regimens

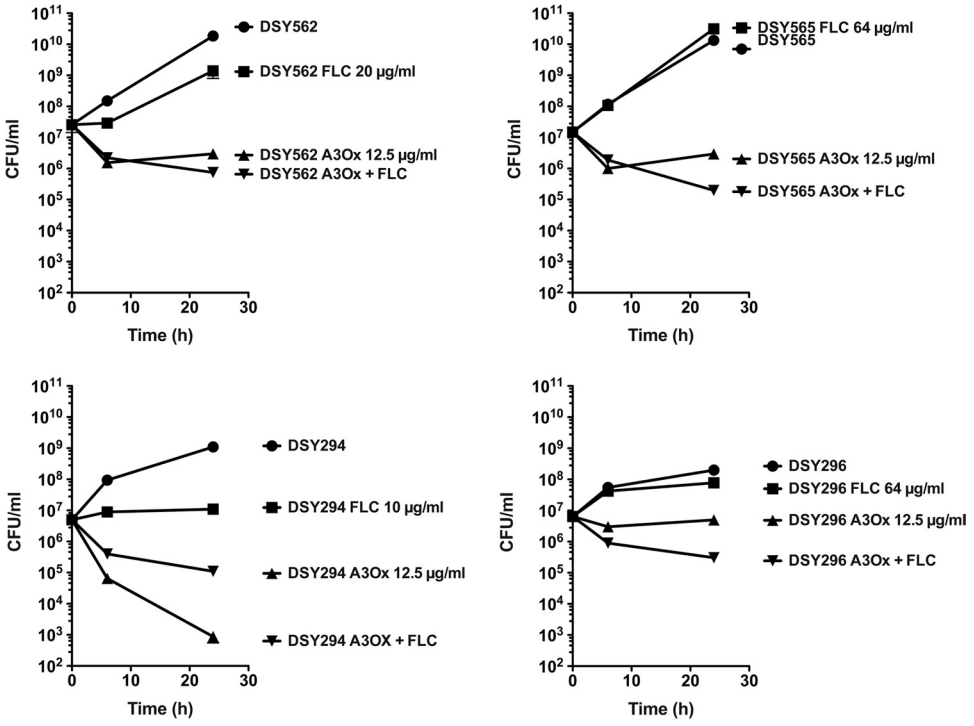

FIG 4 Time-kill curves of A3Ox in *C. glabrata* and *C. albicans*. Each value is the mean of two separate experiments.

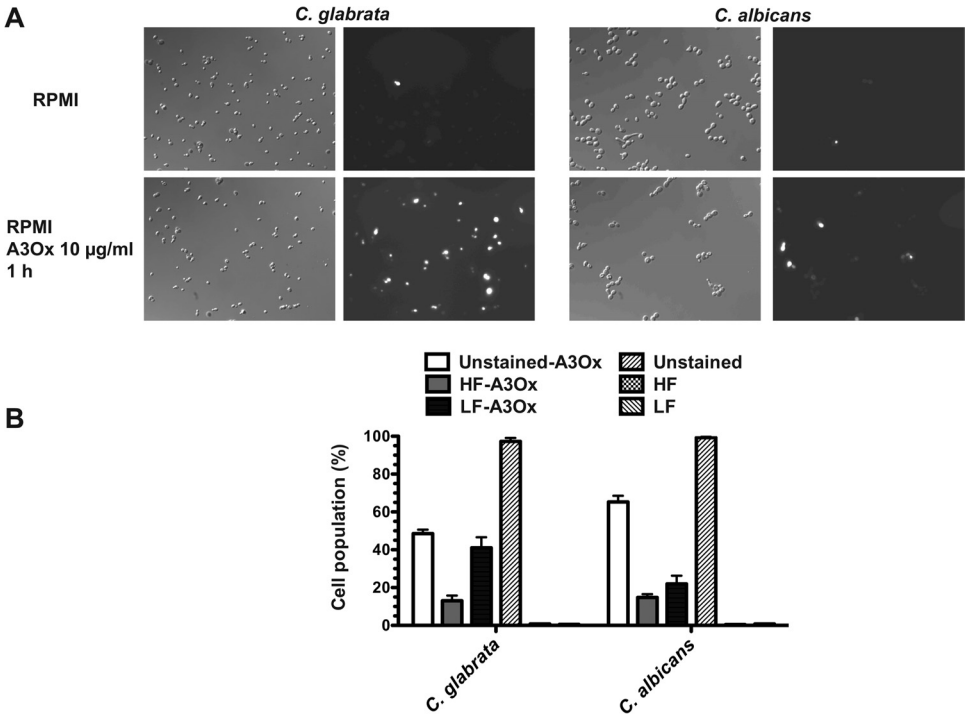

FIG 5 ROS production following A3Ox treatment. (A) Microscopy pictures of *C. glabrata* and *C. albicans* under phase contrast and under fluorescence. The cells were incubated with RPMI or RPMI containing 10 µg of A3Ox/ml at 35°C under constant shaking. Next, the cells were stained with MitoSOX Red (2.5 µg/ml) for 20 min at room temperature, centrifuged, and washed two times with PBS and observed under microscopy. Cells with high fluorescence (HF) are dead cells, while those with low fluorescence (LF) produce ROS. (B) Quantification of MitoSOX Red staining. Approximately 200 cells were counted for each experimental condition (untreated and A3Ox treated).

were applied; however, only the 2.5-mg/kg/day results are shown in Fig. 7 (the 0.5-mg/kg/day results are shown in Fig. S3 in the supplemental material). Fluconazole was used at a dosage of 3 mg/kg/day. As in the case of *C. glabrata*, single drug regimen reduced CFU counts in selected organs, with the exception of fluconazole treatment of the azole-resistant isolate DSY296, which could be expected. Combining both drugs resulted in a sharp decrease of CFU counts of the azole-resistant isolate (Fig. 7). This

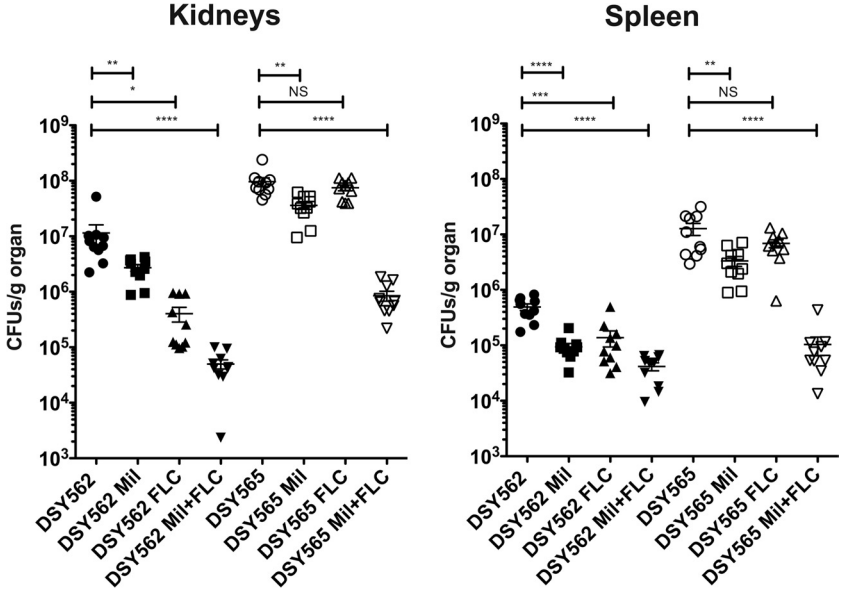

FIG 6 Fungal tissue burdens of mice infected with *C. glabrata* DSY562 and DSY565 and treated with fluconazole (FLC) and commercial milbemycins (Mil: A3Ox/A4Ox mix, 2.5:7.5) or their combination. The regimens for milbemycin and FLC were 2.5 and 100 mg/kg/day, respectively. Each data point corresponds to one animal, and the origin of tissue (kidney or spleen) is shown for each diagram. Geometric means are indicated by horizontal bars, and asterisks indicate statistically significant differences (*, $P < 0.05$; **, $P < 0.01$; ***, $P < 0.001$; ****, $P < 0.0001$). NS, no significance ($P > 0.05$). CFU counts were analyzed with nonparametric Wilcoxon rank-sum tests.

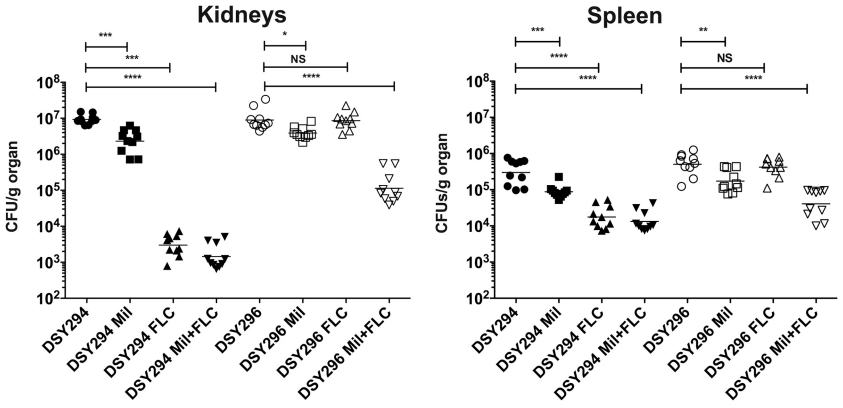

FIG 7 Fungal tissue burdens of mice infected with *C. albicans* DSY294 and DSY296 and treated with fluconazole (FLC) and commercial milbemycins (Mil: A3Ox/A4Ox mix, 2.5:7.5) or their combination. The regimens for milbemycin and FLC were 2.5 and 100 mg/kg/day, respectively. Each data point corresponds to one animal, and the origin of tissue (kidney or spleen) is shown for each diagram. Other figure details are explained in Fig. 6.

combination was however as efficient as the single azole regimen for the azole-susceptible isolate DSY294.

Microarray analysis of milbemycin exposure in *C. albicans* and *C. glabrata*. In order to better understand the effect of milbemycin on *C. albicans* and *C. glabrata*, we subjected both yeast species (azole-susceptible isolates) to a 1-h treatment at supra-MICs (10 μg/ml) to clearly observe their effects and analyzed their transcriptome by microarrays. The conventional laboratory *C. albicans* isolate SC5314 was chosen in these experiments to enable transcriptomic comparisons with experimental data from other laboratories. SC5314 also exhibited the same A3Ox MIC values than DSY294 (Table 3, 6.4 μg/ml). A 2-fold variation in any gene as a result of A3Ox exposure was used as regulation threshold. Microarray data were validated by qPCR with a few genes in *C. albicans* and *C. glabrata* (see Fig. S4 in the supplemental material).

***C. glabrata*.** A3Ox treatment resulted in a 2-fold gene expression variation for 887 genes (421 up- and 466 downregulated genes, respectively). GO term analysis of upregulated genes revealed enrichment of genes involved in oxido-reductive processes and sulfur amino acid biosynthesis (see File S1 in the supplemental material). This observation is consistent with ROS production induced by A3Ox. This was also confirmed by the upregulation of cytochrome *c* oxidase subunits (*COX13*, *COX5B*, and *COX7*), which participate to ROS production from electron transport activities (36). Strikingly, among the most upregulated genes were those encoding heat shock proteins (*SSA3*, *HSP104*, *HSP42*, and *HSP30*) and *BNT2* encoding for a v-SNARE binding protein that facilitates specific protein retrieval from a late endosome to the Golgi. Together with the expression of the above-mentioned chaperones, *BNT2* has been shown to be upregulated in stressed cells in *S. cerevisiae* to promote the sorting of misfolded proteins (37). In relation with this observation, several genes involved in protein ubiquitination (*UBI4*, *UBP7*, *UBP9*, *UBX3*, and *UBX7*) were upregulated by A3Ox treatment. Thus, this expression profile confirms that A3Ox imposes a stress in *C. glabrata*, which itself perturbs protein processing. As a matter of fact, several genes implicated in protein targeting to the vacuole (*VPS* genes) were upregulated by A3Ox treatment, including *VPS8*, *VPS70*, *VPS38*, *VPS27*, and *VPS21*. VPS genes are part of ESCRT system and are involved in the degradation of ubiquitylated proteins via the formation of multivesicular bodies (38).

We also observed that several genes of the calcineurin pathway were upregulated by A3Ox treatment, including *CCH1*, *MID2* *CMK2*, *CRZ1*, and *CMP2*. The calcineurin pathway has been shown to be critical for responding to chemical stress in several yeast species and thus upregulation of this system might represent a mechanism by which *C. glabrata* protects itself against A3Ox toxicity (5, 39, 40). Interestingly, A3Ox treatment seems to upregulate several peroxisomal enzymes (*PEX13*, *PEX18*, and *PEX6*) and among them those involved in the glyoxylate cycle (ÌCL1 and *MLS1*).

***C. albicans*.** A3Ox treatment resulted in a 2-fold gene expression variation for 1,809 genes (1,438 up- and 371 downregulated genes, respectively), thus indicating large perturbations of this substance in the *C. albicans* transcriptome. GO term analysis of upregulated genes showed enrichment of genes involved in proteolytic and ubiquitination processes and involving proteasome assembly (see File S2 in the supplemental material). Thus, A3Ox treatment had a similar outcome as in *C. glabrata* reflecting a stress situation and enhancement of protein degradation. GO terms analysis of upregulated genes revealed enrichments in genes involved mitochondrial electron transport (*NAD6*, *NAD1*, *NAD2*, *NAD3*, *NAD4*, *NAD5*, and *NAD4*). The fact that the mitochondrial electron transport chain is stimulated upon A3Ox treatment and that cytochrome *c* oxidase subunits *COX2* and *COX3B*, as well as the mitochondrial F1F0 ATP synthase subunits *ATP6*, *ATP8*, and *ATP9*, were upregulated may be related to a stimulus of mitochondrial respiration and consequent ROS production in *C. albicans* as described above measured. Consistent with these ob-

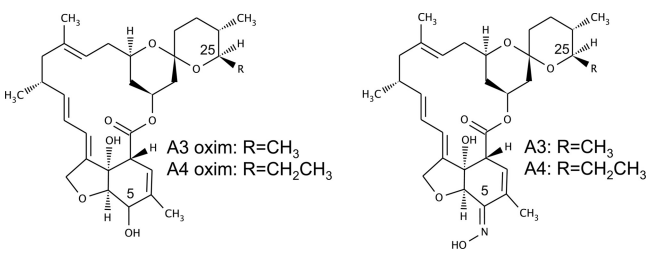

FIG 8 Chemical structures of milbemycins A3/A4 (left) and oxim derivatives (right).

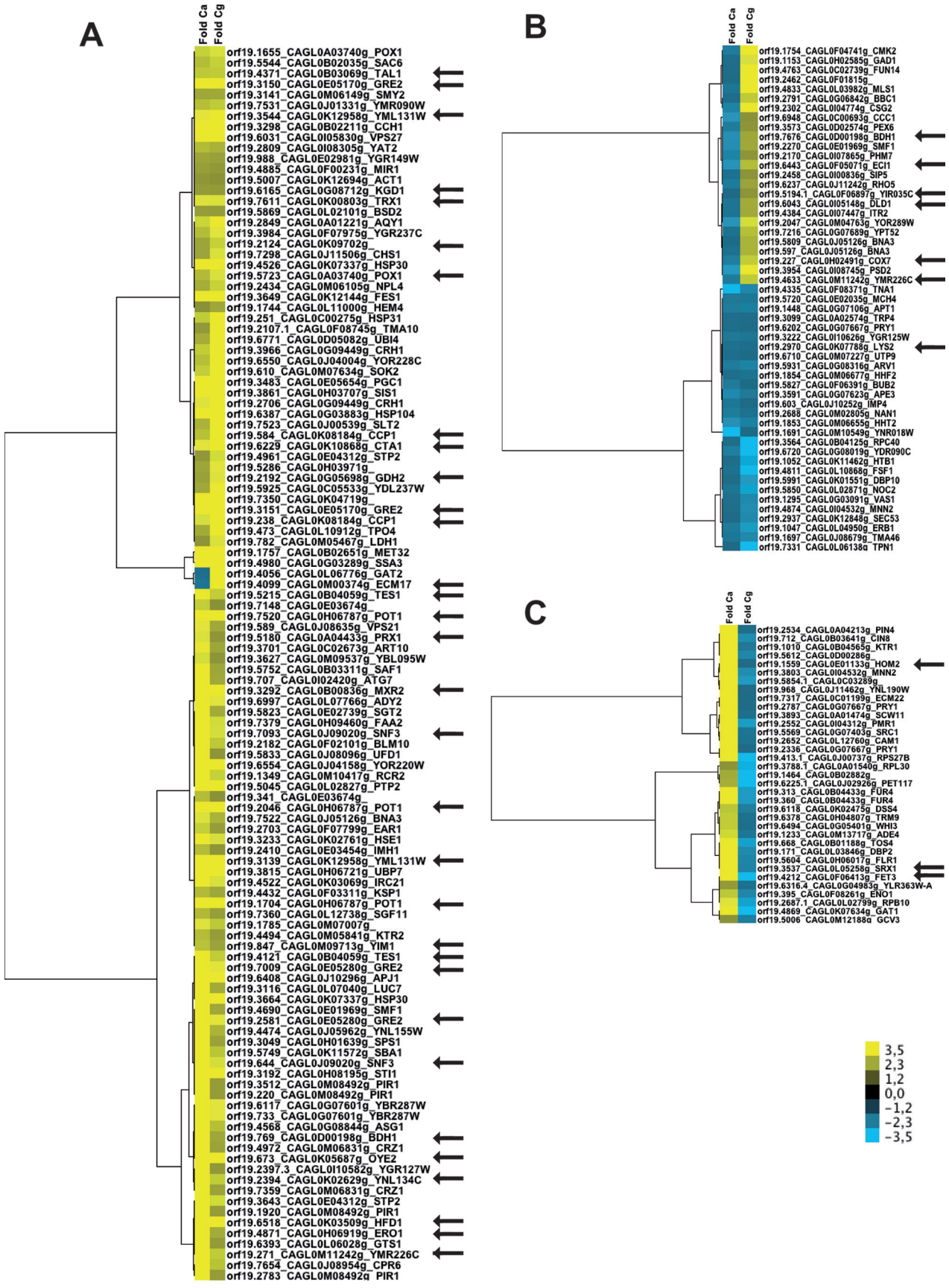
A
Fold Ca
Fold Cg
orf19.1655_CAGL0A03740g_POX1
orf19.5544_CAGL0B02035g_SAC6
orf19.4371_CAGL0B03069g_TAL1
orf19.3150_CAGL0E05170g_GRE2
orf19.3141_CAGL0M06149g_SMY2
orf19.7531_CAGL0J01331g_YMR090W
orf19.3544_CAGL0K12958g_YML131W
orf19.3298_CAGL0B02211g_CCH1
orf19.6031_CAGL0I05830g_VPS27
orf19.2809_CAGL0I08305g_YAT2
orf19.988_CAGL0E02981g_YGR149W
orf19.4885_CAGL0F00231g_MIR1
orf19.5007_CAGL0K12694g_ACT1
orf19.6165_CAGL0G08712g_KGD1
orf19.7611_CAGL0K00803g_TRX1
orf19.5869_CAGL0L02101g_BSD2
orf19.2849_CAGL0A01221g_AQY1
orf19.3984_CAGL0F07975g_YGR237C
orf19.2124_CAGL0K09702g_
orf19.7298_CAGL0J11506g_CHS1
orf19.4526_CAGL0K07337g_HSP30
orf19.5723_CAGL0A03740g_POX1
orf19.2434_CAGL0M06105g_NPL4
orf19.3649_CAGL0K12144g_FES1
orf19.1744_CAGL0L11000g_HEM4
orf19.251_CAGL0C00275g_HSP31
orf19.2107.1_CAGL0F08745g_TMA10
orf19.6771_CAGL0D05082g_UBI4
orf19.3966_CAGL0G09449g_CRH1
orf19.6550_CAGL0J04004g_YOR228C
orf19.610_CAGL0M07634g_SOK2
orf19.3483_CAGL0E05654g_PGC1
orf19.3861_CAGL0H03707g_SIS1
orf19.2706_CAGL0G09449g_CRH1
orf19.6387_CAGL0G03883g_HSP104
orf19.7523_CAGL0J00539g_SLT2
orf19.584_CAGL0K08184g_CCP1
orf19.6229_CAGL0K10868g_CTA1
orf19.4961_CAGL0E04312g_STP2
orf19.5286_CAGL0H03971g_
orf19.2192_CAGL0G05698g_GDH2
orf19.5925_CAGL0C05533g_YDL237W
orf19.7350_CAGL0K04719g_
orf19.3151_CAGL0E05170g_GRE2
orf19.238_CAGL0K08184g_CCP1
orf19.473_CAGL0L10912g_TPO4
orf19.782_CAGL0M05467g_LDH1
orf19.1757_CAGL0B02651g_MET32
orf19.4980_CAGL0G03289g_SSA3
orf19.4056_CAGL0L06776g_GAT2
orf19.4099_CAGL0M00374g_ECM17
orf19.5215_CAGL0B04059g_TES1
orf19.7148_CAGL0E03674g_
orf19.7520_CAGL0H06787g_POT1
orf19.589_CAGL0J08635g_VPS21
orf19.5180_CAGL0A04433g_PRX1
orf19.3701_CAGL0C02673g_ART10
orf19.3627_CAGL0M09537g_YBL095W
orf19.5752_CAGL0B03311g_SAF1
orf19.707_CAGL0I02420g_ATG7
orf19.3292_CAGL0B00836g_MXR2
orf19.6997_CAGL0L07766g_ADY2
orf19.5823_CAGL0E02739g_SGT2
orf19.7379_CAGL0H09460g_FAA2
orf19.7093_CAGL0J09020g_SNF3
orf19.2182_CAGL0F02101g_BLM10
orf19.5833_CAGL0J08096g_UFD1
orf19.6554_CAGL0J04158g_YOR220W
orf19.1349_CAGL0M10417g_RCR2
orf19.5045_CAGL0L02827g_PTP2
orf19.341_CAGL0E03674g_
orf19.2046_CAGL0H06787g_POT1
orf19.7522_CAGL0J05126g_BNA3
orf19.2703_CAGL0F07799g_EAR1
orf19.3233_CAGL0K02761g_HSE1
orf19.2410_CAGL0E03454g_IMH1
orf19.3139_CAGL0K12958g_YML131W
orf19.3815_CAGL0H06721g_UBP7
orf19.4522_CAGL0K03069g_IRC21
orf19.4432_CAGL0F03311g_KSP1
orf19.1704_CAGL0H06787g_POT1
orf19.7360_CAGL0L12738g_SGF11
orf19.1785_CAGL0M07007g_
orf19.4494_CAGL0M05841g_KTR2
orf19.847_CAGL0M09713g_YIM1
orf19.4121_CAGL0B04059g_TES1
orf19.7009_CAGL0E05280g_GRE2
orf19.6408_CAGL0J10296g_APJ1
orf19.3116_CAGL0L07040g_LUC7
orf19.3664_CAGL0K07337g_HSP30
orf19.4690_CAGL0E01969g_SMF1
orf19.2581_CAGL0E05280g_GRE2
orf19.4474_CAGL0J05962g_YNL155W
orf19.3049_CAGL0H01639g_SPS1
orf19.5749_CAGL0K11572g_SBA1
orf19.644_CAGL0J09020g_SNF3
orf19.3192_CAGL0H08195g_STI1
orf19.3512_CAGL0M08492g_PIR1
orf19.220_CAGL0M08492g_PIR1
orf19.6117_CAGL0G07601g_YBR287W
orf19.733_CAGL0G07601g_YBR287W
orf19.4568_CAGL0G08844g_ASG1
orf19.769_CAGL0D00198g_BDH1
orf19.4972_CAGL0M06831g_CRZ1
orf19.673_CAGL0K05687g_OYE2
orf19.2397.3_CAGL0I10582g_YGR127W
orf19.2394_CAGL0K02629g_YNL134C
orf19.7359_CAGL0M06831g_CRZ1
orf19.3643_CAGL0E04312g_STP2
orf19.1920_CAGL0M08492g_PIR1
orf19.6518_CAGL0K03509g_HFD1
orf19.4871_CAGL0H06919g_ERO1
orf19.6393_CAGL0L06028g_GTS1
orf19.271_CAGL0M11242g_YMR226C
orf19.7654_CAGL0J08954g_CPR6
orf19.2783_CAGL0M08492g_PIR1
B
Fold Ca
Fold Cg
orf19.1754_CAGL0F04741g_CMK2
orf19.1153_CAGL0H02585g_GAD1
orf19.4763_CAGL0C02739g_FUN14
orf19.2462_CAGL0F01815g_
orf19.4833_CAGL0L03982g_MLS1
orf19.2791_CAGL0G06842g_BBC1
orf19.2302_CAGL0I04774g_CSG2
orf19.6948_CAGL0C00693g_CCC1
orf19.3573_CAGL0D02574g_PEX6
orf19.7676_CAGL0D00198g_BDH1
orf19.2270_CAGL0E01969g_SMF1
orf19.2170_CAGL0I07865g_PHM7
orf19.6443_CAGL0F05071g_ECI1
orf19.2458_CAGL0I00836g_SIP5
orf19.6237_CAGL0J11242g_RHO5
orf19.5194.1_CAGL0F06897g_YIR035C
orf19.6043_CAGL0I05148g_DLD1
orf19.4384_CAGL0I07447g_ITR2
orf19.2047_CAGL0M04763g_YOR289W
orf19.7216_CAGL0G07689g_YPT52
orf19.5809_CAGL0J05126g_BNA3
orf19.597_CAGL0J05126g_BNA3
orf19.227_CAGL0H02491g_COX7
orf19.3954_CAGL0I08745g_PSD2
orf19.4633_CAGL0M11242g_YMR226C
orf19.4335_CAGL0F08371g_TNA1
orf19.5720_CAGL0E02035g_MCH4
orf19.1448_CAGL0G07106g_APT1
orf19.3099_CAGL0A02574g_TRP4
orf19.6202_CAGL0G07667g_PRY1
orf19.3222_CAGL0I10626g_YGR125W
orf19.2970_CAGL0K07788g_LYS2
orf19.6710_CAGL0M07227g_UTP9
orf19.5931_CAGL0G08316g_ARV1
orf19.1854_CAGL0M06677g_HHF2
orf19.5827_CAGL0F06391g_BUB2
orf19.3591_CAGL0G07623g_APE3
orf19.603_CAGL0J10252g_IMP4
orf19.2688_CAGL0M02805g_NAN1
orf19.1853_CAGL0M06655g_HHT2
orf19.1691_CAGL0M10549g_YNR018W
orf19.3564_CAGL0B04125g_RPC40
orf19.6720_CAGL0G08019g_YDR090C
orf19.1052_CAGL0K11462g_HTB1
orf19.4811_CAGL0L10868g_FSF1
orf19.5991_CAGL0K01551g_DBP10
orf19.5850_CAGL0L02871g_NOC2
orf19.1295_CAGL0G03091g_VAS1
orf19.4874_CAGL0I04532g_MNN2
orf19.2937_CAGL0K12848g_SEC53
orf19.1047_CAGL0L04950g_ERB1
orf19.1697_CAGL0J08679g_TMA46
orf19.7331_CAGL0L06138g_TPN1
C
Fold Ca
Fold Cg
orf19.2534_CAGL0A04213g_PIN4
orf19.712_CAGL0B03641g_CIN8
orf19.1010_CAGL0B04565g_KTR1
orf19.5612_CAGL0D00286g_
orf19.1559_CAGL0E01133g_HOM2
orf19.3803_CAGL0I04532g_MNN2
orf19.5854.1_CAGL0C03289g_
orf19.968_CAGL0J11462g_YNL190W
orf19.7317_CAGL0C01199g_ECM22
orf19.2787_CAGL0G07667g_PRY1
orf19.3893_CAGL0A01474g_SCW11
orf19.2552_CAGL0I04312g_PMR1
orf19.5569_CAGL0G07403g_SRC1
orf19.2652_CAGL0L12760g_CAM1
orf19.2336_CAGL0G07667g_PRY1
orf19.413.1_CAGL0J00737g_RPS27B
orf19.3788.1_CAGL0A01540g_RPL30
orf19.1464_CAGL0B02882g_
orf19.6225.1_CAGL0J02926g_PET117
orf19.313_CAGL0B04433g_FUR4
orf19.360_CAGL0B04433g_FUR4
orf19.6118_CAGL0K02475g_DSS4
orf19.6378_CAGL0H04807g_TRM9
orf19.6494_CAGL0G05401g_WHI3
orf19.1233_CAGL0M13717g_ADE4
orf19.668_CAGL0B01188g_TOS4
orf19.171_CAGL0L03846g_DBP2
orf19.5604_CAGL0H06017g_FLR1
orf19.3537_CAGL0L05258g_SRX1
orf19.4212_CAGL0F06413g_FET3
orf19.6316.4_CAGL0G04983g_YLR363W-A
orf19.395_CAGL0F08261g_ENO1
orf19.2687.1_CAGL0L02799g_RPB10
orf19.4869_CAGL0K07634g_GAT1
orf19.5006_CAGL0M12188g_GCV3
3,5
2,3
1,2
0,0
−1,2
−2,3
−3,5

servations, orf19.148, orf19.639.1, and orf19.2438 (encoding for mitochondrial large ribosomal subunits *MRPL31*, *MRPL44*, and *MRPS12*, respectively) were upregulated in A3Ox-treated cells. We observed that upregulated genes were also enriched in oxidoreductive functions, especially those related to peroxide detoxification (*URE2*, *CCP1*, *GTT12*, orf19.4436, *PRX1*, *DOT5*, orf19.584, *TTR1*, *CAT1*, *TSA1*, and *GPX1*), probably reflecting the enhanced mitochondrial activity upon A3Ox treatment. GO terms analysis of upregulated genes also revealed enrichments in genes involved in cell wall biogenesis, including, for example, *DIT1*, *PHR3*, *PHR2*, *CSK1*, *CHS2*, *CDA2*, and *ROM2*. Several genes encoding GPI-anchored proteins (*PGA11*, *PGA14*, *PGA15*, *PGA17*, *PGA19*, *PGA22*, *PGA23*, *PGA25*, *PGA27*, *PGA28*, *PGA30*, *PGA31*, *PGA39*, *PGA41*, *PGA42*, *PGA44*, *PGA46*, *PGA49*, *PGA58*, *PGA60*, and *PGA63*) were also upregulated by A3Ox treatment. We noticed that *MKC1* encoding for a mitogen-activated protein (MAP) kinase involved in cell wall integrity was upregulated by A3Ox, thus raising the possibility that A3Ox is sensed by the cell wall integrity pathway, the activation of which results in upregulation of several cell wall genes, including those above listed (41). Interestingly, several genes encoding heat shock and chaperone proteins (*ASR1*, *HSP104*, *HSP30*, *HSP31*, and *HSP70*) were upregulated upon A3Ox treatment and thus highlight that *C. albicans* is under stress as in the case of *C. glabrata*.

Intriguingly, we noticed a strong upregulation of *WOR1*, a master regulator of white-opaque switching in *C. albicans* (42) upon A3Ox treatment. White and opaque cells show dramatic differences in terms of cell shape, gene expression profile, drug permeability, and virulence (42–46). It is known that ectopic expression of this master regulator in the background of *C. albicans* isolates homozygous for the mating type locus (*MTL***a** or *MTL*α) results in a massive conversion of white cells to the opaque state (47). We found that 50 of 214 genes upregulated in the opaque phase as published by Tsong et al. (46) were also upregulated by A3Ox. Normally, *WOR1* is repressed in the strain SC5314 (which was used here in microarray experiments) heterozygote for the mating locus but this repression can be released by inhibition of the **a**1/α2 homeobox transcriptional complex. Thus, A3Ox was capable to release this complex directly or indirectly and thus favored the upregulation of *WOR1* and its targets. We verified that A3Ox could induce white-opaque switching using a A3Ox disk assay onto Lee's medium. Opaque cells could be observed around the disk zone, thus confirming that A3Ox could stimulate white-opaque switching (see Fig. 4S in the supplemental material). The stimulation of the opaque state upon exposure to toxic environments has been documented in the past (48). This stimulation is the consequence of growth inhibition in the background of cells homozygous for the mating locus (48).

Other genes regulated by A3Ox treatment were reminiscent of stress conditions consequent of exposure to exogenous toxic compounds: we noticed upregulation of genes involved in DNA repair (*RAD* genes), upregulation of *MCA1*, a caspase-like gene, and also genes involved in drug resistance such as the transcription factor *MRR1*. The upregulation of *MRR1* is accompanied by upregulation of some of its target genes (35 out of 84 target genes), among which *MDR1*, a multidrug transporter of the major facilitator family (49). *MRR1* upregulation by A3Ox is consistent with a response of *C. albicans* to metabolic inhibitors.

DISCUSSION

In this work, we demonstrated that milbemycins are effective agents to treat *C. albicans* and *C. glabrata* infections in combination with fluconazole in animal models and even reverse azole resistance to levels of wild-type isolates. We showed that milbemycins A3 and A4 and especially their oxim derivatives have potent drug efflux inhibition activities. Several studies already established that this family of substances inhibit fungal ABC transporters (20, 21, 50); however, it is the first time, to our knowledge, that this is demonstrated for oxim derivatives. These substances are active components of commercial antiparasitic drugs and thus are easy to obtain in large quantities.

One of the most remarkable properties of milbemycin oxims was their antifungal and fungicidal activities both in *C. albicans* and *C. glabrata*, which to our knowledge has not been reported yet for other efflux inhibitors. This activity seems to be mediated by the oxim prosthetic group, since A4 and A3 were not exhibiting the same activity. Furthermore, A3Ox was the most potent compound in both *Candida* species. Thus, both the difference in chemical structure between A3 and A4 (Fig. 8, one ethyl and methyl group at position 25, respectively) and the addition of an oxim group (Fig. 8, at position 5) (51) conferred a strong antifungal activity. Milbemycin oxims carry two activities, one including the inhibition of drug efflux at low concentration (efflux inhibition was detectable starting from 0.1 μg/ml) and the other including antifungal activity at higher drug concentrations (3.2 to 6.4 μg/ml). The antifungal activity is independent of the presence or absence of ABC transporters, since mutants lacking major ABC transporters involved in azole resistance (CgCdr1/CgCdr2, Cdr1, and Cdr2) exhibit similar A3Ox MIC values to wild-type isolates (data not shown). Interestingly, efflux inhibition is more potent against drug-resistant *C. albicans* than *C. glabrata*, as reflected by the respective inhibition of R6G efflux (V_{max} IC_{50}s are >20-fold higher for *C. glabrata*, Fig. 2). This is possibly due to structural differences of ABC transporters between the two species which may result in different inhibitor affinities. The intrinsic antifungal activity of A3Ox, on the other hand, shows no difference between the two types of isolates, therefore highlighting that it is mediated by an ABC-transporter-independent mechanism of action.

With the idea to better understand how the fungicidal effect of A3Ox was exerted on *C. albicans* and *C. glabrata*, we performed whole-genome transcript profiling with the same drug concentration and experiment duration. The results obtained revealed, as expected, several features common to drug stress that include the mobilization of oxidoreductive processes, of chaperoning of mis-

FIG 9 Cluster analysis of coregulated and ortholog genes between *C. albicans* and *C. glabrata*. Gene orthologues were obtained from data available at *Candida* Genome database (CGD) and were extracted from data available on Files S1 and S3 in the supplemental material. Genes were clustered with the CLUSTER 3.0 software using centroid linkage preset. The data were viewed with TreeView (version 1.1.6r2). Gene symbols contain the *C. albicans* with the corresponding *C. glabrata* ortholog and the attached gene name. Three subclusters are shown. (A) Genes upregulated in *C. albicans* and *C. glabrata*; (B) genes downregulated in *C. albicans* and down-/upregulated in *C. glabrata*; (C) genes upregulated in *C. albicans* and downregulated in *C. glabrata*. "Fold-Ca" and "Fold-Cg" indicate the fold change expression in the presence of A3Ox compared to untreated controls. Arrows indicate genes assigned by GO term analysis to oxidoreductive processes (see File S3 in the supplemental material for details). The colored scale corresponds to the fold changes in gene expression ranging from <3.5-fold to >3.5-fold.

folded proteins and of protein degradation pathways. The upregulation of the caspase-like gene *MCA1* in *C. albicans* could be related to the fungicidal effect of A3Ox. It has been shown that a striking caspase activity pattern can occur in *C. albicans* during oxidative stress-induced programmed cell death (PCD) (52). Together with the ROS-producing activity of A3Ox, *MCA1* upregulation suggests that A3Ox has the capacity to induce PCD in *C. albicans*, although it can be expected that cell necrosis would be an important readout of A3Ox exposure.

One surprising observation was the apparent divergent transcriptional response of both *Candida* species upon A3Ox exposure. We found that 204 gene orthologs between *C. glabrata* (of 887 genes) and *C. albicans* (of 1,809 genes) were commonly regulated by A3Ox, which reflects a common response mechanism, but also demonstrated quite different effects of this drug on the transcriptome of the two yeast species (see File S3 in the supplemental material). The cluster analysis of these 204 regulated genes showed that 62 were regulated in the opposite way between the two yeast species (Fig. 9). The remaining genes that were commonly up- and downregulated could constitute a common core of genes responding to A3Ox in a species-independent way. The GO term analysis of the 144 coregulated genes revealed enrichments of genes involved in oxidoreductive processes and in oxidative stress response, which is consistent with a stress situation (see File S3 in the supplemental material). From the annotated genes involved in oxidoreductive processes, 75% belonged to genes commonly upregulated by A3Ox between both species (Fig. 9). Oxidative stress is a signature common in response to xenobiotics in yeast (53–55), and our transcript profile analyses therefore underline a similar effect for A3Ox. In addition to this oxidative stress response, the presence of chaperone genes (HSP gene family), of genes involved in protein ubiquitination process, and of genes involved in ESCRT vesicle trafficking was reminiscent of the response signature involving protein damage (55). Interestingly, MAP kinases from both *C. albicans* (*MKC1*) and *C. glabrata* (*SLT2*) were also upregulated upon A3Ox treatment. Besides the role of these kinases in cell wall integrity as described above, it has been suggested that at least *MKC1* participates to oxidative stress response (56), which is again in agreement with the idea that A3Ox stress responses involve oxidative processes.

At this stage, it is not possible to predict direct cellular targets of this substance in addition to efflux transporters in the tested *Candida* isolates. A few studies comparing the effect of the same drug on different yeast species using microarrays are available. These studies have investigated the effect of antifungal drugs on fungal metabolism and generally could identify common response patterns between the different investigated species (1). Here, we identified a limited overlap of gene expression between *C. glabrata* and *C. albicans*, thus suggesting species-specific response signatures. This could be due to the evolutionary distance between both yeast species, which determines how a specific pathogen behaves in contact with exogenous substances. However, even if species are more closely related, drug response can be still different as illustrated by transcriptome comparisons between *C. glabrata* and *S. cerevisiae* in the presence of benomyl (57). The same conclusion was drawn for the response of diverse yeast species to azoles (58).

Testing efflux inhibitors in animal models has been achieved in a few occasions. For example, Hayama et al. (59) have used the D-octapeptide derivative RC21v3, a Cdr1 inhibitor, in the treatment of murine oral candidiasis caused by azole-susceptible and azole-resistant *C. albicans* clinical isolates. RC21v3 potentiated the therapeutic efficacy of fluconazole for mice infected with either strain. Sorensen et al. (60) reported that milbemycin α_9 could potentiate fluconazole in an experimental systemic pyelonephritis with *C. albicans*. We showed here that milbemycin oxims could potentiate fluconazole efficacy both in *C. albicans* and *C. glabrata* using a systemic model of infection, and thus we expand the concept of drug combination to both of these important fungal pathogens. We have used different milbemycin regimens ranging from 0.5 to 2.5 mg/kg/day in mice without signs of toxicity. These dosages correspond to those given in animal care (61). A higher dosage (5 mg/kg/day) exhibited slight toxicity effects in treated mice without increasing fluconazole efficacy (data not shown). The serum levels obtained after 7-day treatments reached concentrations near to the MIC measured in *C. glabrata* and *C. albicans*. This could explain why milbemycin oxims on their own could decrease fungal burden in tissues infected with *C. glabrata* and *C. albicans*. On the other hand, we have shown in previous studies that the ABC transporter *CgCDR1* could participate to *C. glabrata* virulence (23). Thus, inhibition of this transporter by milbemycins could also impact on *C. glabrata* virulence and therefore could contribute to the decrease of tissue burden upon inhibitor treatment.

Whether or not milbemycin oxims with fluconazole can be used in human is an open question. The primary targets of the substance are glutamate sensitive chloride channels in neurons and myocytes of invertebrates, leading to hyperpolarization of these cells and blocking of signal transfer. These glutamate channels are specific for invertebrates and are not expressed in mammalian hosts (62). Some milbemycin derivatives have been used in humans already. For example, Cotreau et al. (63) reported the use of moxidectin to treat onchocerciasis (river blindness). Onchocerciasis is a parasitic disease caused by the helminth *Onchocerca volvulus* and is transmitted to humans through the bite of a black fly of the genus *Simulium*. This study showed that such substances have low toxicity in humans when administered in the 3- to 36-mg range. Our preliminary data show that moxidectin acts synergistically with fluconazole in *C. glabrata* and *C. albicans* as in the case of milbemycin A3Ox. Therefore, the use of milbemycin for treating *Candida* infections is potentially possible in humans. *Candida* infections, and especially *C. glabrata* infections, are rising in diverse countries and, together with azole resistance levels reached nowadays by *C. glabrata*, alternative therapeutic approaches should be proposed in the future (4).

ACKNOWLEDGMENTS

We are indebted to Françoise Ischer for technical assistance and Alix Coste for stimulating discussion. We also thank Sandra Schorderet-Weber and Jacques Bouvier (Novartis Animal Health) for discussions and help for providing milbemycin derivatives.

This study was partially supported by a grant from the Swiss Research National Foundation 31003A_127378 and from a Swiss-Indo Collaborative Research grant ISJRP 122917.

REFERENCES

1. **Sanglard D, Coste A, Ferrari S.** 2009. Antifungal drug resistance mechanisms in fungal pathogens from the perspective of transcriptional gene regulation. FEMS Yeast Res. **9**:1029–1050.
2. **Pfaller MA.** 2012. Antifungal drug resistance: mechanisms, epidemiology, and consequences for treatment. Am. J. Med. **125**:S3–S13.
3. **Pfaller MA, Diekema DJ.** 2012. Progress in antifungal susceptibility test-

ing of *Candida* spp. using Clinical and Laboratory Standards Institute broth microdilution methods, 2010–2012. J. Clin. Microbiol. **50**:2846–2856.
4. **Lockhart SR, Iqbal N, Ahlquist AM, Farley MM, Harrison LH, Bolden CB, Baughman W, Stein B, Hollick R, Park BJ, Chiller T.** 2012. Species identification and antifungal susceptibility of *Candida* bloodstream isolates from population-based surveillance in two US cities: 2008–2011. J. Clin. Microbiol. **50**:3435–3442.
5. **Shapiro RS, Robbins N, Cowen LE.** 2011. Regulatory circuitry governing fungal development, drug resistance, and disease. Microbiol. Mol. Biol. Rev. **75**:213–267.
6. **Sanglard D, Ischer F, Calabrese D, Majcherczyk PA, Bille J.** 1999. The ATP binding cassette transporter gene *CgCDR1* from *Candida glabrata* is involved in the resistance of clinical isolates to azole antifungal agents. Antimicrob. Agents Chemother. **43**:2753–2765.
7. **Sanglard D, Ischer F, Bille J.** 2001. Role of ATP-binding-cassette transporter genes in high-frequency acquisition of resistance to azole antifungals in *Candida glabrata*. Antimicrob. Agents Chemother. **45**:1174–1183.
8. **Torelli R, Posteraro B, Ferrari S, La Sorda M, Fadda G, Sanglard D, Sanguinetti M.** 2008. The ATP-binding cassette transporter-encoding gene CgSNQ2 is contributing to the CgPDR1-dependent azole resistance of *Candida glabrata*. Mol. Microbiol. **68**:186–201.
9. **Ferrari S, Ischer F, Calabrese D, Posteraro B, Sanguinetti M, Fadda G, Rohde B, Bauser C, Bader O, Sanglard D.** 2009. Gain of function mutations in *CgPDR1* of *Candida glabrata* not only mediate antifungal resistance but also enhance virulence. PLoS Pathog. **5**:e1000268. doi:10.1371/journal.ppat.1000268.
10. **Tsai H, Krol A, Sarti K, Bennett J.** 2006. *Candida glabrata* PDR1, a transcriptional regulator of a pleiotropic drug resistance network, mediates azole resistance in clinical isolates and petite mutants. Antimicrob. Agents Chemother. **50**:1384–1392.
11. **Vermitsky J-P, Earhart KD, Smith WL, Homayouni R, Edlind TD, Rogers PD.** 2006. Pdr1 regulates multidrug resistance in *Candida glabrata*: gene disruption and genome-wide expression studies. Mol. Microbiol. **61**:704–722.
12. **Tsai H, Sammons L, Zhang X, Suffis S, Su Q, Myers T, Marr K, Bennett J.** 2010. Microarray and molecular analyses of the azole resistance mechanism in *Candida glabrata* oropharyngeal isolates. Antimicrob. Agents Chemother. **54**:3308–3317.
13. **Caudle KE, Barker KS, Wiederhold NP, Xu L, Homayouni R, Rogers PD.** 2011. Genomewide expression profile analysis of the *Candida glabrata* Pdr1 regulon. Eukaryot. Cell **10**:373–383.
14. **Coste AT, Karababa M, Ischer F, Bille J, Sanglard D.** 2004. TAC1, transcriptional activator of CDR genes, is a new transcription factor involved in the regulation of *Candida albicans* ABC transporters CDR1 and CDR2. Eukaryot. Cell **3**:1639–1652.
15. **Coste AT, Crittin J, Bauser C, Rohde B, Sanglard D.** 2009. Functional analysis of *cis*- and *trans*-acting elements of the *Candida albicans* CDR2 promoter with a novel promoter reporter system. Eukaryot. Cell **8**:1250–1267.
16. **Dunkel N, Blass J, Rogers P, Morschhauser J.** 2008. Mutations in the multidrug resistance regulator MRR1, followed by loss of heterozygosity, are the main cause of MDR1 overexpression in fluconazole-resistant *Candida albicans* strains. Mol. Microbiol. **69**:827–840.
17. **Heilmann C, Schneider S, Barker K, Rogers P, Morschhauser J.** 2010. An A643T mutation in the transcription factor Upc2p causes constitutive ERG11 upregulation and increased fluconazole resistance in *Candida albicans*. Antimicrob. Agents Chemother. **54**:353–359.
18. **Hoot SJ, Smith AR, Brown RP, White TC.** 2011. An A643V amino acid substitution in Upc2p contributes to azole resistance in well-characterized clinical isolates of *Candida albicans*. Antimicrob. Agents Chemother. **55**:940.
19. **Whiteway M.** 2012. Seeking antifungal drug synergies. Microbe **7**:234–237.
20. **Niimi K, Harding D, Parshot R, King A, Lun D, Decottignies A, Niimi M, Lin S, Cannon R, Goffeau A, Monk B.** 2004. Chemosensitization of fluconazole resistance in *Saccharomyces cerevisiae* and pathogenic fungi by a D-octapeptide derivative. Antimicrob. Agents Chemother. **48**:1256–1271.
21. **Cannon RD, Lamping E, Holmes AR, Niimi K, Baret PV, Keniya MV, Tanabe K, Niimi M, Goffeau A, Monk BC.** 2009. Efflux-mediated antifungal drug resistance. Clin. Microbiol. Rev. **22**:291–321.
22. **Anderson JB.** 2005. Evolution of antifungal-drug resistance: mechanisms and pathogen fitness. Nat. Rev. Microbiol. **3**:547–556.
23. **Ferrari S, Sanguinetti M, Torelli R, Posteraro B, Sanglard D.** 2011. Contribution of CgPDR1-regulated genes in enhanced virulence of azole-resistant *Candida glabrata*. PLoS One **6**:e17589. doi:10.1371/journal.pone.0017589.
24. **Gillum AM, Tsay EY, Kirsch DR.** 1984. Isolation of the *Candida albicans* gene for orotidine-5′-phosphate decarboxylase by complementation of *S. cerevisiae ura3* and *E. coli pyrF* mutations. Mol. Gen. Genet. **198**:179–182.
25. **Maccallum DM, Coste A, Ischer F, Jacobsen MD, Odds FC, Sanglard D.** 2010. Genetic dissection of azole resistance mechanisms in *Candida albicans* and their validation in a mouse model of disseminated infection. Antimicrob. Agents Chemother. **54**:1476–1483.
26. **Coste A, Selmecki A, Forche A, Diogo D, Bougnoux M-E, D'enfert C, Berman J, Sanglard D.** 2007. Genotypic evolution of azole resistance mechanisms in sequential *Candida albicans* isolates. Eukaryot. Cell **6**:1889–1904.
27. **Singh A, Prasad R.** 2011. Comparative lipidomics of azole sensitive and resistant clinical isolates of *Candida albicans* reveals unexpected diversity in molecular lipid imprints. PLoS One **6**:e19266. doi:10.1371/journal.pone.0039812.
28. **Subcommittee on Antifungal Susceptibility Testing (AFST) of the ESCMID European Committee for Antimicrobial Susceptibility Testing (EUCAST).** 2008. EUCAST definitive document EDef 7.1: method for the determination of broth dilution MICs of antifungal agents for fermentative yeasts. Clin. Microbiol. Infect. **14**:398–405.
29. **Te Dorsthorst DTA, Verweij PE, Meletiadis J, Bergervoet M, Punt NC, Meis JFGM, Mouton JW.** 2002. In vitro interaction of flucytosine combined with amphotericin B or fluconazole against thirty-five yeast isolates determined by both the fractional inhibitory concentration index and the response surface approach. Antimicrob. Agents Chemother. **46**:2982–2989.
30. **Maesaki S, Marichal P, Vanden Bossche H, Sanglard D, Kohno S.** 1999. Rhodamine 6G efflux for the detection of CDR1-overexpressing azole-resistant *Candida albicans* strains. J. Antimicrob. Chemother. **44**:27–31.
31. **Synnott JM, Guida A, Mulhern-Haughey S, Higgins DG, Butler G.** 2010. Regulation of the hypoxic response in *Candida albicans*. Eukaryot. Cell **9**:1734–1746.
32. **Ferrari S, Sanguinetti M, De Bernardis F, Torelli R, Posteraro B, Vandeputte P, Sanglard D.** 2011. Loss of mitochondrial functions associated with azole resistance in *Candida glabrata* results in enhanced virulence in mice. Antimicrob. Agents Chemother. **55**:1852–1860.
33. **Vandeputte P, Pradervand S, Ischer F, Coste AT, Ferrari S, Harshman K, Sanglard D.** 2012. Identification and functional characterization of Rca1, a transcription factor involved in both antifungal susceptibility and host response in *Candida albicans*. Eukaryot. Cell **11**:916–931.
34. **Dryden M, Payne P.** 2005. Preventing parasites in cats. Vet. Ther. **6**:260–267.
35. **Batova M, Klobucnikova V, Oblasova Z, Gregan J, Zahradnik P, Hapala I, Subik J, Schüller C.** 2010. Chemogenomic and transcriptome analysis identifies mode of action of the chemosensitizing agent CTBT (7-chlorotetrazolo[5,1-c]benzo[1,2,4]triazine). BMC Genomics **11**:153.
36. **Bender T, Leidhold C, Ruppert T, Franken S, Voos W.** 2010. The role of protein quality control in mitochondrial protein homeostasis under oxidative stress. Proteomics **10**:1426–1443.
37. **Malinovska L, Kroschwald S, Munder MC, Richter D, Alberti S.** 2012. Molecular chaperones and stress-inducible protein sorting factors coordinate the spatio-temporal distribution of protein aggregates. Mol. Biol. Cell **23**:3041–3056.
38. **Fabrizio P, Hoon S, Shamalnasab M, Galbani A, Wei M, Giaever G, Nislow C, Longo VD.** 2010. Genome-wide screen in *Saccharomyces cerevisiae* identifies vacuolar protein sorting, autophagy, biosynthetic, and tRNA methylation genes involved in life span regulation. PLoS Genet. **6**:e1001024.
39. **Chen YL, Konieczka JH, Springer DJ, Bowen SE, Zhang J, Silao FG, Bungay AA, Bigol UG, Nicolas MG, Abraham SN, Thompson DA, Regev A, Heitman J.** 2012. Convergent evolution of calcineurin pathway roles in thermotolerance and virulence in *Candida glabrata*. G3 (Bethesda) **2**:675–691.
40. **Sanglard D, Ischer F, Marchetti O, Entenza J, Bille J.** 2003. Calcineurin A of *Candida albicans*: involvement in antifungal tolerance, cell morphogenesis and virulence. Mol. Microbiol. **48**:959–976.

41. **Monge RA, Roman E, Nombela C, Pla J.** 2006. The MAP kinase signal transduction network in *Candida albicans*. Microbiology **152**:905–912.
42. **Zordan RE, Galgoczy DJ, Johnson AD.** 2006. Epigenetic properties of white-opaque switching in *Candida albicans* are based on a self-sustaining transcriptional feedback loop. Proc. Natl. Acad. Sci. U. S. A. **103**:12807–12812.
43. **Lohse MB, Johnson AD.** 2009. White-opaque switching in *Candida albicans*. Curr. Opin. Microbiol. **12**:650–654.
44. **Alby K, Jr.** 2009. To switch or not to switch?: Phenotypic switching is sensitive to multiple inputs in a pathogenic fungus. Commun. Integr. Biol. **2**:509–511.
45. **Lohse MB, Johnson AD.** 2008. Differential phagocytosis of white versus opaque *Candida albicans* by *Drosophila* and mouse phagocytes. PLoS One **3**:e1473. doi:10.1371/journal.pone.0001473.
46. **Tsong AE, Miller MG, Raisner RM, Johnson AD.** 2003. Evolution of a combinatorial transcriptional circuit: a case study in yeasts. Cell **115**:389–399.
47. **Huang G, Wang H, Chou S, Nie X, Chen J, Liu H.** 2006. Bistable expression of WOR1, a master regulator of white-opaque switching in *Candida albicans*. Proc. Natl. Acad. Sci. U. S. A. **103**:12813–12818.
48. **Alby K, Bennett RJ.** 2009. Stress-induced phenotypic switching in *Candida albicans*. Mol. Biol. Cell **20**:3178–3191.
49. **Morschhauser J, Barker K, Liu T, Bla B, Homayouni R, Rogers P.** 2007. The transcription factor Mrr1p controls expression of the MDR1 efflux pump and mediates multidrug resistance in *Candida albicans*. PLoS Pathog. **3**:e164. doi:10.1371/journal.ppat.0030164.
50. **Holmes A, Lin Y, Niimi K, Lamping E, Keniya M, Niimi M, Tanabe K, Monk B, Cannon R.** 2008. ABC transporter Cdr1p contributes more than Cdr2p does to fluconazole efflux in fluconazole-resistant *Candida albicans* clinical isolates. Antimicrob. Agents Chemother. **52**:3851–3862.
51. **Shoop WL, Mrozik H, Fisher MH.** 1995. Structure and activity of avermectins and milbemycins in animal health. Vet. Parasitol. **59**:139–156.
52. **Cao Y, Huang S, Dai B, Zhu Z, Lu H, Dong L, Cao Y, Wang Y, Gao P, Chai Y, Jiang Y.** 2009. *Candida albicans* cells lacking CaMCA1-encoded metacaspase show resistance to oxidative stress-induced death and change in energy metabolism. Fungal Genet. Biol. **46**:183–189.
53. **Santos PM, Simões T, Sá-Correia I.** 2009. Insights into yeast adaptive response to the agricultural fungicide mancozeb: a toxicoproteomics approach. Proteomics **9**:657–670.
54. **Dias PJ, Teixeira MC, Telo JP, Sá-Correia I.** 2010. Insights into the mechanisms of toxicity and tolerance to the agricultural fungicide mancozeb in yeast, as suggested by a chemogenomic approach. OMICS **14**:211–227.
55. **dos Santos SC, Teixeira MC, Cabrito TR, Sá-Correia I.** 2012. Yeast toxicogenomics: genome-wide responses to chemical stresses with impact in environmental health, pharmacology, and biotechnology. Front. Genet. **3**:63.
56. **de Dios CH, Roman E, Monge RA, Pla J.** 2010. The role of MAPK signal transduction pathways in the response to oxidative stress in the fungal pathogen *Candida albicans*: implications in virulence. Curr. Protein Pept. Sci. **11**:693–703.
57. **Lelandais G, Tanty V, Geneix C, Etchebest C, Jacq C, Devaux F.** 2008. Genome adaptation to chemical stress: clues from comparative transcriptomics in *Saccharomyces cerevisiae* and *Candida glabrata*. Genome Biol. **9**:R164.
58. **Kuo D, Tan K, Zinman G, Ravasi T, Bar-Joseph Z, Ideker T.** 2010. Evolutionary divergence in the fungal response to fluconazole revealed by soft clustering. Genome Biol. **11**:R77.
59. **Hayama K, Ishibashi H, Ishijima SA, Niimi K, Tansho S, Ono Y, Monk BC, Holmes AR, Harding DR, Cannon RD, Abe S.** 2012. A D-octapeptide drug efflux pump inhibitor acts synergistically with azoles in a murine oral candidiasis infection model. FEMS Microbiol. Lett. **328**:130–137.
60. **Sorensen K, Corcoran E, Huie K, Chen S, Tembe V, Griffith D, Lomovskaya O, Watkins W, Dudley NM.** 2000. *In vivo* potentiation of fluconazole by the fungal efflux pump inhibitor MC-510,011 in a mouse model of pyelonephritis due to fluconazole-susceptible and -resistant *Candida albicans*, abstr 1502, p 209. Abstr. 40th Intersci. Conf. Antimicrob. Agents Chemother., Toronto, Ontario, Canada.
61. **Tranquilli WJ, Paul AJ, Todd KS.** 1991. Assessment of toxicosis induced by high-dose administration of milbemycin oxime in collies. Am. J. Vet. Res. **52**:1170–1172.
62. **Cully DF, Vassilatis DK, Liu KK, Paress PS, Van der Ploeg LH, Schaeffer JM, Arena JP.** 1994. Cloning of an avermectin-sensitive glutamate-gated chloride channel from *Caenorhabditis elegans*. Nature **371**:707–711.
63. **Cotreau MM.** 2003. The antiparasitic moxidectin: safety, tolerability, and pharmacokinetics in humans. J. Clin. Pharmacol. **43**:1108–1115.